NRIAG Journal of Astronomy and Geophysics (2016) 5, 65–75

National Research Institute of Astronomy and Geophysics

NRIAG Journal of Astronomy and Geophysics

www.elsevier.com/locate/nrjag

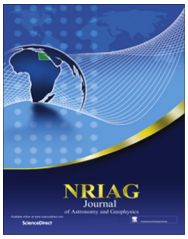

Evaluation of the deformation parameters of the northern part of Egypt using Global Navigation Satellite System (GNSS)

Abdel-Monem S. Mohamed [a], Ali M. Radwan [a,*], Mohamed Sharf [b], Zakaria Hamimi [b], Esraa E. Hegazy [b], Nadia Abou Aly [a], Mahmoud Gomaa [a]

[a] *National Research Institute of Astronomy and Geophysics, Egypt*
[b] *Geology Department, Faculty of Science, Benha University, Benha 13518, Egypt*

Received 11 October 2015; revised 22 December 2015; accepted 3 January 2016
Available online 14 January 2016

KEYWORDS

Tectonic setting;
Crustal deformation;
Seismic activity;
Northern Egypt

Abstract The northern part of Egypt is a rapidly growing development accompanied by the increased levels of standard living particularly in its urban areas. From tectonic and seismic point of views, the northern part of Egypt is one of the interested regions. It shows an active geologic structure attributed to the tectonic movements of the African and Eurasian plates from one side and the Arabian plate from the other side. From historical point of view and recent instrumental records, the northern part of Egypt is one of the seismo-active regions in Egypt. The investigations of the seismic events and their interpretations had led to evaluate the seismic hazard for disaster mitigation, for the safety of the densely populated regions and the vital projects. In addition to the monitoring of the seismic events, the most powerful technique of Global Navigation Satellite System (GNSS) will be used in determining crustal deformation where a geodetic network covers the northern part of Egypt. Joining the GPS Permanent stations of the northern part of Egypt with the Southern part of Europe will give a clear picture about the recent crustal deformation and the African plate velocity. The results from the data sets are compared and combined in order to determine the main characteristics of the deformation and hazard estimation for specified regions. Final compiled output from the seismological and geodetic analysis will throw lights upon the geodynamical regime of these seismo-active regions. This work will throw lights upon the geodynamical regime and to delineate the crustal stress and strain fields in the study region. This also enables to evaluate the active tectonics

* Corresponding author at: 1 El-Marsd Str., Dept. of Geodynamics, National Research Institute of Astronomy and Geophysics, 11421 Helwan, Egypt and 61714, El-Gendia Village, Bany-Mazar City, Menia, Egypt. Tel.: +20 2556 0645, +20 01002435750, +20 01002435750 (mobile).
E-mail address: amradwaneg@yahoo.com (A.M. Radwan).

Peer review under responsibility of National Research Institute of Astronomy and Geophysics.

ELSEVIER Production and hosting by Elsevier

http://dx.doi.org/10.1016/j.nrjag.2016.01.001

and surface deformation with their directions from repeated geodetic observations. The results show that the area under study suffers from continuous seismic activity related to the crustal movements taken place along trends of major faults

1. Introduction

Recent crustal deformation studies have a great role for evaluating the geodynamics of the seismo-active regions in any country. The crustal deformation must be put in mind where it connects significantly with the human life and its resources. From a historical point of view and recent instrumental records, there are some seismo-active regions in Egypt where some significant earthquakes had occurred in different places. Special tectonic features in Egypt are the territories of a high seismic risk which has to be monitored using up-to date technologies. Detailed investigations of the seismic events along with interpretations led to evaluate the seismic hazard for disaster mitigation and for the safety of the densely populated regions. The region under study is suffering from moderate earthquakes which occurred in the Mediterranean Sea, the area southwest and southeast of Cairo, North Delta and the area between Cairo-Ismaillia and Cairo-Suez roads. Most of these areas are economically important and strategic regions. In addition to the monitoring of the seismic events, the most powerful technique of satellite geodesy GPS is used for determining the crustal deformation where a geodetic network was established in 2006 covering all territories of Egypt. The active crustal deformation field in the northern part of Egypt is being examined, as obtained from both seismological and GPS data. Results obtained from the data sets are compared and combined in order to determine the main characteristics of deformation and hazard estimation for specified region. The final compiled output from the seismic and geodetic analysis focuses on the geodynamical regime of the area and it is an attempt to delineate the crustal stress and strain fields. The obtained results reveal a clear picture about the crustal deformation and their role in the earthquake occurrence.

2. Tectonic setting

Egypt was affected by the structural elements and tectonics of the northeastern corner of the African plate and the south east of the Mediterranean Sea. It was affected also by the tectonic setting of Sinai Sub-plate and the Gulf of Suez-Red Sea Rift System. Tectonic features of prime importance in the vicinity of Egypt are represented by three major tectonic plate boundaries (Fig. 1): (a) the Africa–Eurasia Plate margin, (b) the Levant Transform Fault and (c) the Red Sea Plate Margin. These margins separate the African, Eurasian and Arabian plates. The Arabian–Nubian Shield and the surrounding shelf area are discriminated into four major geologic provinces (Said, 1962).

The northern part of Egypt underwent three subsequent tectonic phases from early Mesozoic to present. The first tectonic phase is the Neotethys rifting which formed the North Africa Passive Margin in the early Triassic to Early Jurassic with the development of an extensive system of generally E–W trending rift basins located inboard from the continental margin. The second phase is manifested by the NW–SE (to WNW–ESE)-oriented normal faults. During the Late Cretaceous, the relative motion between Africa and Eurasia changed from sinistral divergent to dextral convergent (Savostin et al., 1986; Guiraud and Bosworth, 1997). These compressional events developed a number of inversion-related features including localized folding and wrench faulting, igneous activity and associated episodes of uplifting, erosion and offshore deposition. The deformation effect extends from Libya to the Levant. A train of ENE folding accompanied with thrust faults (Syrian Arc Structure) and NW to NNW extension faults parallel to the major contraction force was developed from the eastern region of the Western Desert (Sehim, 1993) and across Sinai (Moustafa and Khalil, 1990).

The latest tectonic phase started from the Late Eocene and continued up to recent times and is dominated by three fault trends. The first one is represented by the NNW-oriented Gulf of Suez normal faults in Late Eocene–Miocene. The second is manifested by the NNE-trending faults that are related to the development of the Gulf of Aqaba rift that started to form since the Miocene by left lateral oblique slip movement. The third one comprises the N–S fault trend (Moustafa et al., 1998).

3. Seismic activity

Territory of Egypt is not a major seismic zone, but earthquakes represent a significant hazard. Most of the earthquake activity is associated with the tectonic features along the margins of these plates. Many historical and recent earthquakes occurred in the Red Sea, Gulf of Suez and Gulf of Aqaba regions. The interaction of the African, Arabian, Eurasian plates and Sinai sub-plate is the main factor of the seismicity of the northern part of Egypt. Fig. 2 shows the distribution of earthquakes foci for the period from 1997 to 2014 and Fig. 3 illustrates the seismic activity during the geodetic observations for the period 2011–2014. It is clear that there is no significant earthquake taken place at the Nile Delta area while most of the significant earthquakes have taken place at the intersection between the Mediterranean and Red seas fault trend.

4. Earthquake focal mechanisms

Earthquake source mechanisms are of prime importance in monitoring local, regional and global seismicity. They reflect the stress pattern acting in the area under study and may help to map its tectonic structure which causes an earthquake. A

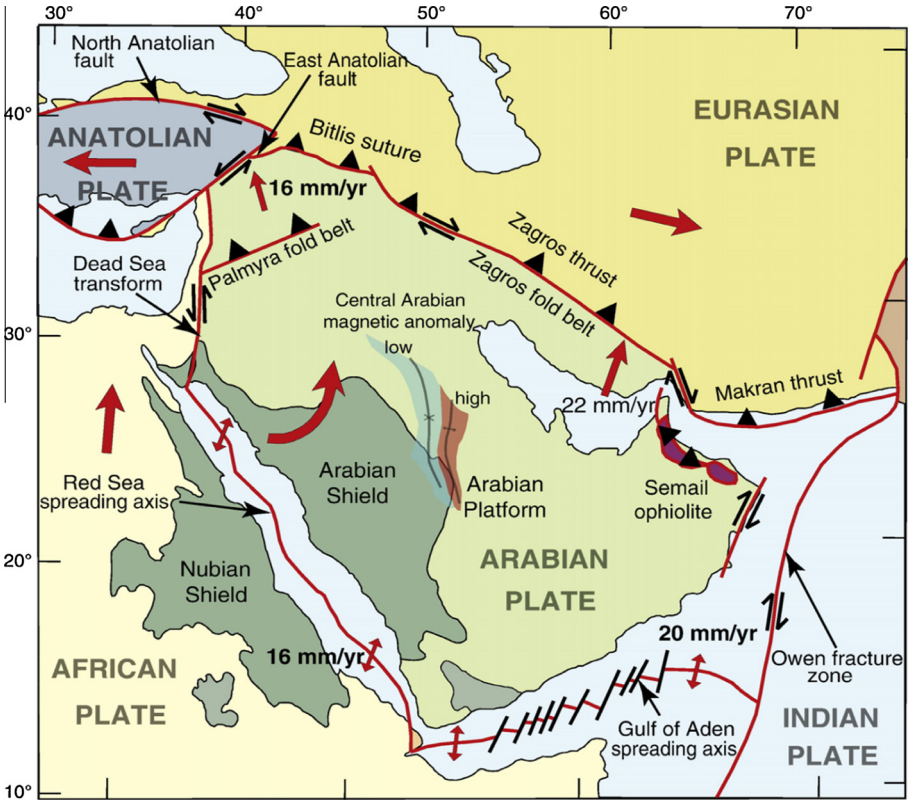

Figure 1 Simplified map of the Arabian plate, with plate boundaries, approximate plate convergence vectors and principal geologic features (after Stern and Johnson, 2010).

Focal Mechanism Solution (FMS) is the result of an analysis of waveforms generated by an earthquake and recorded by a number of seismographs. It usually takes at least 10 records to produce a reasonable FMS. The complete characterization of an earthquake's focal mechanism provides important information including the origin time, epicenter location, focal depth, seismic moment (a direct measure of the energy released by an earthquake), magnitude and spatial orientation of the 9 components of the moment tensor. From the moment tensor, orientation and sense of slip of the fault can ultimately be resolved. This wealth of information about an earthquake is plainly of interest to a structural geologist working on active structures. Fault plane solutions can be made by several methods such as *p*-wave directions, surface wave and the spectral amplitude of the body waves. Almost all investigations can use the direction of the first *p*-wave in the earthquake focal mechanism studies.

The data compiled from seismograms of the ENSN in a digital format. These data are extracted from remote sites online to the ring buffer using Atlas program (version 1.2). A relocation analysis of the selected seismic events during the period from 2011 to 2014 was done using HYPOINVERSE program after picking both the arrival times of *P* and *S* wave when available. Also, the impulsive and emergent *P*-wave polarities are picked. The focal mechanisms of events have been done using the polarities (compression or dilatation) of the first motion of *P* waves. The solutions are carried out using the software package developed by Suetsugu (1995).

In the present study, we have selected the largest events which occurred during the study period to solve the focal mechanism on them. The parameters of events used for focal mechanism solution are listed in Tables 1 and 2 and Fig. 4. The Suez–Cairo shear zone is affected by several earthquakes within the studied time interval but the earthquakes selected are four.

In the western desert of Egypt, the epicenter of the events is situated at the unstable shelf which is characterized by relatively thick sedimentary sequence underlain by high basement relief due to block faulting and affected by minor compressional folding. They are located at the northern part of the western desert (Dahshour area) and its surrounding Wadi El-Natrun. Focal mechanism of event No (1) reflects normal faulting mechanism with minor strike slip fault and its nodal planes trending E–W to NW–SE. The mechanism of event No (2) reveals normal faulting with large strike slip component and its nodal plane NW–SE to NE–SW; so it gives *T*-axis directed NNW–SSE. Several earthquakes are occurred in the Gulf of Suez area during the studied time, but one evident earthquake has been selected for focal mechanism. The focal mechanism of event No (3) reflects a normal fault with slightly strike slip component and its nodal plane trending WNW–ESE. All rupture planes are directed parallel to the Gulf of Suez and the main trend of *T*-axis along the Gulf of Suez is NNW–SSE which is consistent with the dominant tension stress along the Gulf of Suez.

The area to southeast of Cairo along the Suez–Cairo shear zone (Hagul and Kottamia), the northeast Cairo (Abu Za'abal area) and other regions (Beni-Suef region) are represented by several events. The Suez–Cairo shear zone is affected by several earthquakes within the studied time interval but the evi-

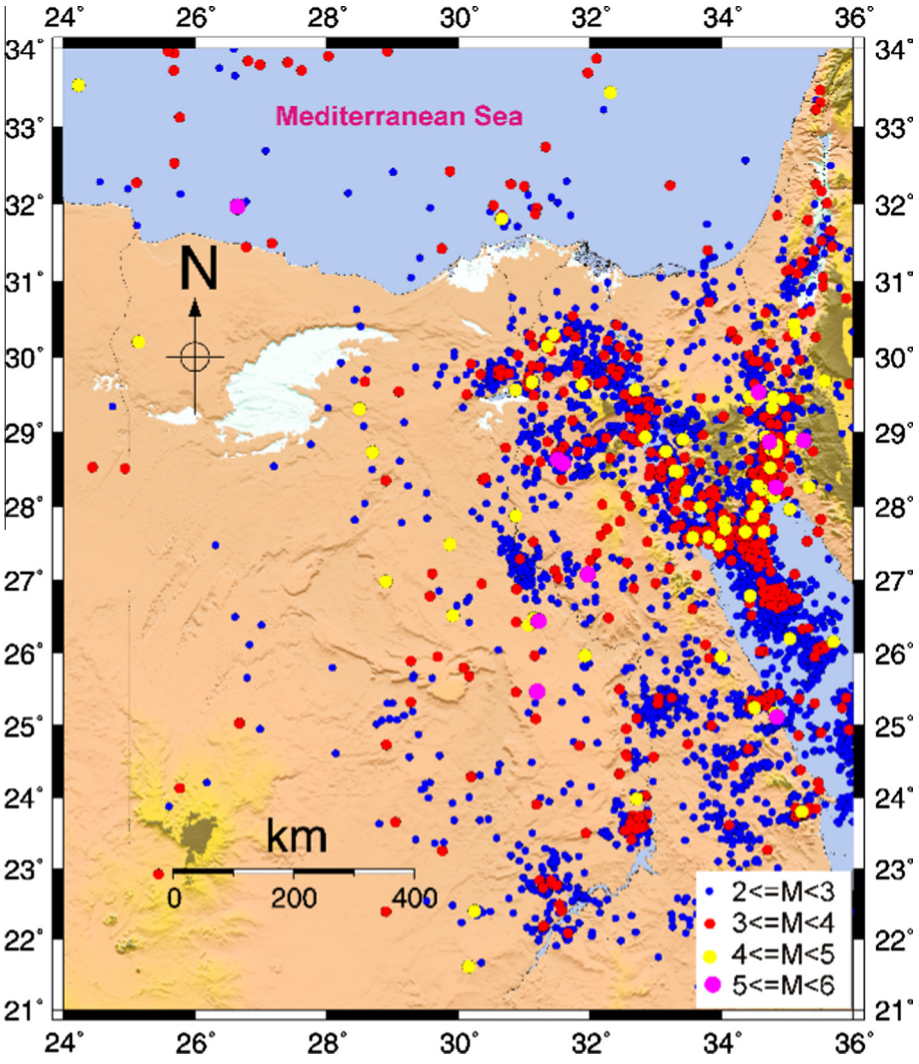

Figure 2 Seismicity of Egypt recorded by Egyptian National Seismic Network (ENSN) for the period from 1997 to 2014.

dent earthquakes that have been selected are three. The solutions of event No (4) show a normal faulting mechanism and its nodal plane trending NE–SW and WNW–ESE. The solution of events No (6 & 7) at Hagul area indicates a normal faulting with strike-slip component along nodal plane trending NE–SW and NW–SE. Only one event is selected in Sinai Peninsula area due to the very little scarily occurrences of earthquakes during the study time. The focal mechanism solution of event No (5) displays a normal fault with strike-slip component, and its nodal planes are trending NW–SE and NE–SW (see Figs. 5 and 7).

5. Egyptian Permanent GPS Network (EPGN)

In 2006, the National Research Institute of Astronomy and Geophysics (NRIAG) started the establishment of the Egyptian Permanent GPS Network (EPGN). Basically, the site selection not only aimed to cover geographically all the Egyptian territories but also considers the tectonic setting and seismic activity of Egypt. Also, the chosen places for constructing these stations fulfilled the required criteria, such as clear view without any obstructions, away from any electromagnetic sources and accessibility. By the end of 2014, the number of this network increased to be 25 stations covering most of the Egyptian territories. Due to the importance of the monumentation type and its quality that affects directly the stability of these stations, the majority of EPGN stations were installed on concrete pillars, but in a few cases, some stations were installed on a roof of building (Saleh and Becker, 2013). GPS network that covers the study area was eight stations in 2007 and extended to be thirteen stations in 2012. The study area lies between 29 to 31.5N and 25 to 33.8E (Table 3 and Fig. 6).

6. Data processing

Data analysis processing was mainly divided into two stages, namely the pre-processing stage and the processing stage. The pre-processing stage includes the following: (1) acquiring the precise ephemeris files and earth orientation parameters and then, convert these files from the terrestrial frame to the celestial reference frame; (2) selecting data of some Interna-

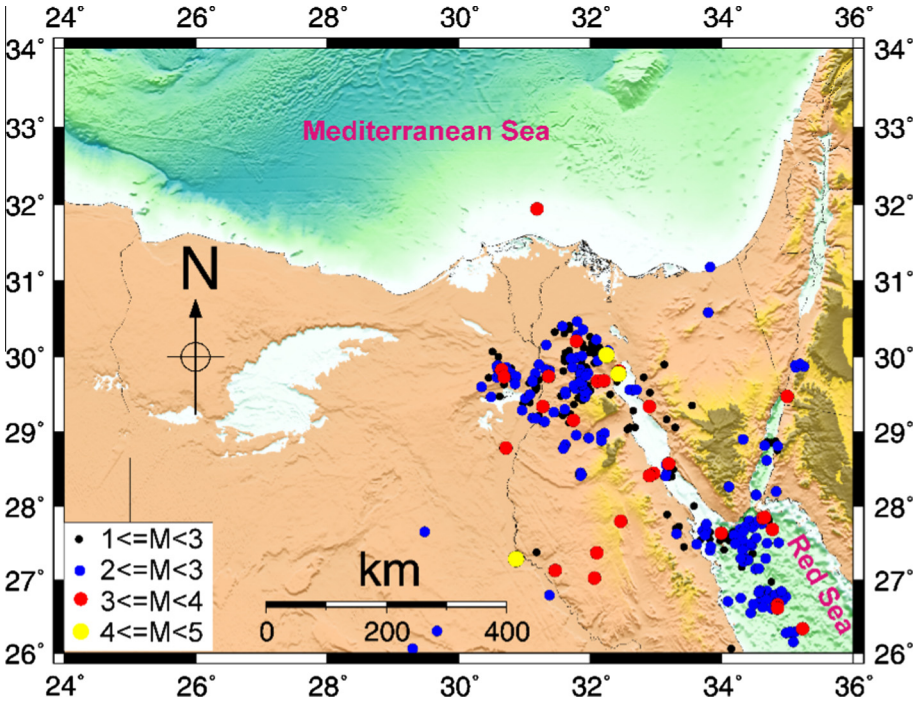

Figure 3 Seismicity of Northern part of Egypt recorded by ENSN during the geodetic observations for the period from 2011 to 2014.

Table 1 Parameters of the events.

No	Date			Time			Location		H	ML
	Y	M	D	H	M	S	Lat.	Long.	(km)	
1	2011	8	5	06	41	33	29.09	31.09	5.17	3.18
2	2012	2	16	02	15	12	29.65	30.66	3.027	3.7
3	2013	3	8	23	20	11	29.15	32.71	3.37	3.34
4	2013	3	25	12	40	40	29.04	32.30	22.06	4.2
5	2014	2	11	09	55	30	29.34	32.93	3.48	3.27
6	2014	7	18	20	01	29	30.01	32.23	24.09	4.2
7	2014	7	22	03	03	44	29.77	32.41	22.49	4.9

Table 2 Focal mechanism parameters of the events.

No	*P*-axis		*T*-axis		Nodal plane 1			Nodal plane 2		
	AZ	PL	AZ	PL	ST	Dip	Rake	ST	Dip	Rake
1	265	55	160	10	44	63	−128	283	45	−40
2	261	23	353	6	39	70	−167	305	78	−21
3	155	39	51	16	288	76	−138	185	50	−19
4	8	82	231	6	327	40	−82	136	51	−97
5	24	2	114	8	159	83	176	249	86	7
6	358	36	263	7	34	60	−23	136	71	−148
7	71	73	−160	11	121	57	−74	274	36	−113

tional GPS Service for Geodynamics (IGS) permanent stations such as "Ankr", "Not1", "Drag" and "BAHR"; (3) Preparing the GPS data for processing, such as transferring these data to RINEX (Receiver Independent Exchange) format.

The processing stage includes the following:Processing the collected data using the Bernese software version 5.2 (Dach et al., 2007), the used Computational Strategy is as follows:

- Reference frame ITRF 2008.
- Velocity model of tectonic plate motion.
- Usage of IGS final orbits and satellite clocks and IGS final Earth orientation parameters.
- Automatic forming of baselines based on OBS-MAX strategy (usage of maximum number of observations) for phase observation processing.

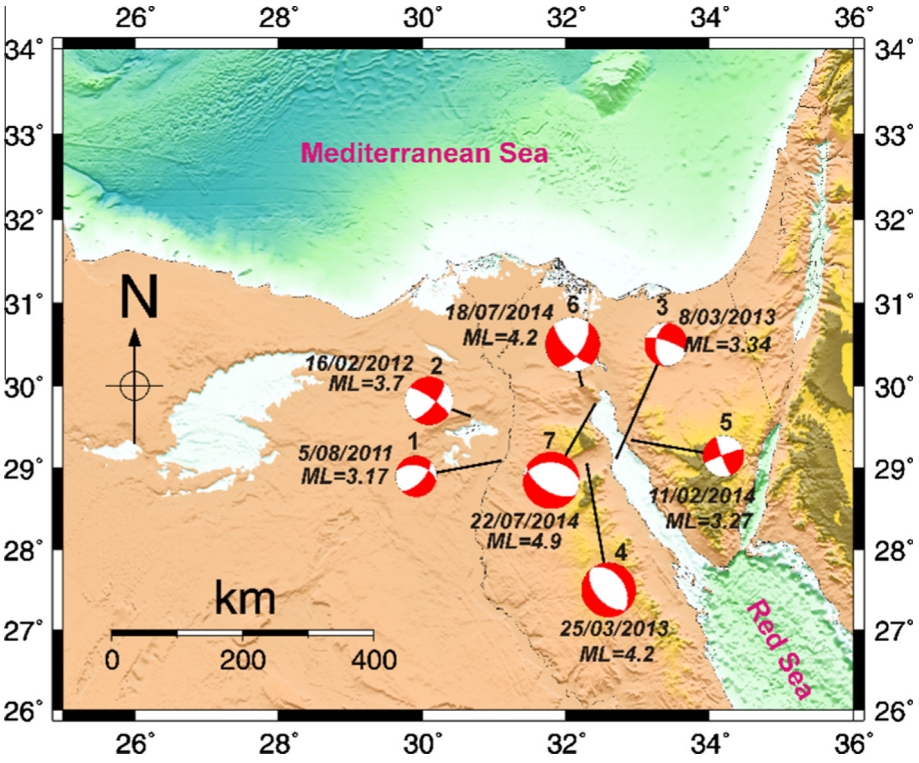

Figure 4 Location of seven events used for focal mechanism analysis.

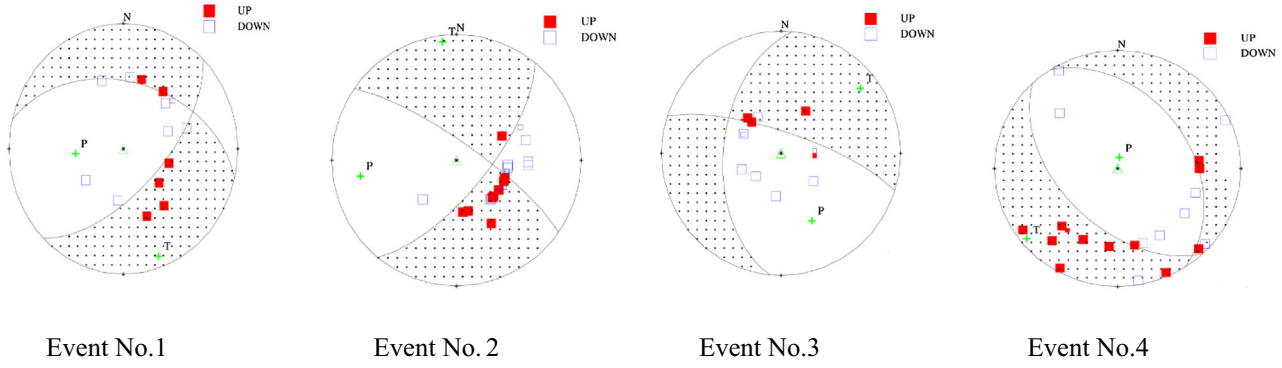

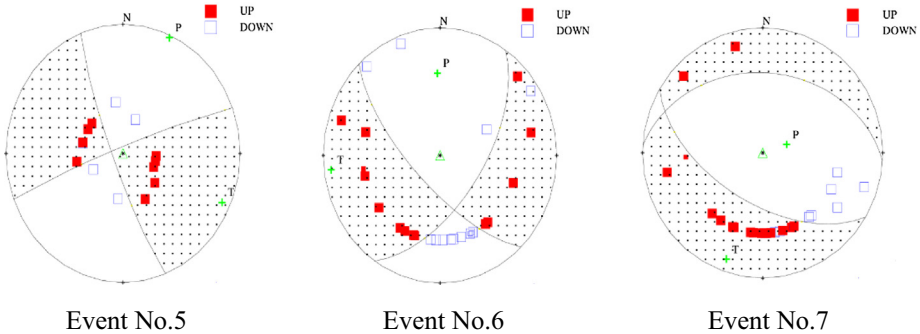

Figure 5 Focal mechanism solutions.

Table 3 Names of stations, their codes (ID) and elevations.

Station name	Codes (ID)	Longitude	Latitude	Elevation (m)
Helwan	1	31.82	29.93	153.639
Mesalat	2	30.89	29.51	153.639
Katamyia	3	31.34	29.86	502.173
Arish	4	33.62	31.11	27.394
Port Said	5	32.31	31.25	41.977
Damietta	6	31.14	31.31	43.599
Gamalyia	7	31.86	31.18	32.4096
Mansoura	8	31.35	31.04	39.588
Hamoul	9	31.68	31.44	23.848
Alexandria	10	29.91	31.20	57.995
Borg Al-Arab	11	29.57	30.86	98.091
Marsa Matrouh	12	27.23	31.35	58.699
Salum	13	25.21	31.49	91.304

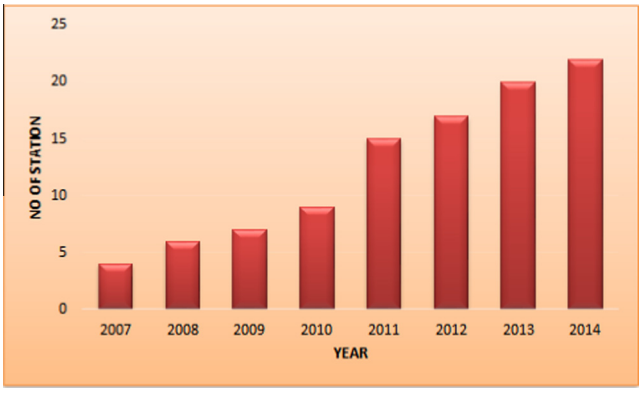

Figure 6 Development of the Egyptian Permanent GPS Network (EPGN).

- Quasi-Ionosphere-Free (QIF) strategy of phase ambiguity resolution.
- Ionosphere-free frequency L3 eliminating the influence of ionosphere.
- Elevation cutoff angle 3°.
- Troposphere model Dry Niell, consideration of mapping function for hourly zenith path delay (Wet Niell) and daily horizontal gradient (tilting).

The displacement vectors at each GPS station were determined under an assumption of free network adjustment. The obtained values were adjusted to get the more accurate positions of the GPS stations. The horizontal components of displacement vectors with 95% confidence error ellipses are shown in Figs. 8 and 9. The error ellipses represent standard error in all directions around the observed site. Fig. 8 and Table 4 show the horizontal movements including the horizontal velocity of the African plate during this period. In order to reveal the local horizontal movements in the study area, the effect of African plat movement has to be removed. By extracting the values of the African plate, deduced from model Nuvell 1A (McClusky et al., 2003), as shown in Table 5 and Fig. 9, the displacement vectors can be mainly attributed to the movement within the study area for those period of observations. It is noticed that the local movements are small which reflect the greater impact of the regional geodynamics rather than the local movements.

7. Deformation parameters estimation

There are numerous applications of crustal deformation studies and the most one is the representation of the deformation in terms of strain parameters. The basic principles of strain analysis, as developed in the theory of elasticity, are applicable, if the area covered by the monitoring network can be considered as a continuum deforming under stress. The infinitesimal homogenous horizontal strain model is used. Vertical strain is not included to avoid the less accuracy in the vertical component (Kakkuri and Chen, 1991). The deformations are generally small in comparison with the size of the network. So, they may be modeled by a differential relationship. Let us denote the strain rate for a line at a point P in the direction $\propto_i$ with the value ε_i (Jaeger, 1964 and Schneider, 1982). The equations are titled as follows: (Abdel-Monem et al., 2011):

$$\varepsilon_i = \frac{\Delta s_i}{\Delta t_i \cdot s_i} = e_{xx}\cos^2\alpha_i + e_{xy}\sin 2\alpha_i + e_{yy}\sin^2\alpha_i$$

where

s_i is the unstrained length of the line computed (ellipsoidal distance),

Δs_i is the change in s_i during the time interval Δt_i.

The rates of the strain tensor components are defined as follows:-

$$e_{xx} = \frac{1}{\Delta t}\cdot\frac{\partial u}{\partial x}$$

$$e_{yy} = \frac{1}{\Delta t}\cdot\frac{\partial v}{\partial y} = e_{xy} = \frac{1}{2\Delta t}\cdot\left(\frac{\partial u}{\partial y} + \frac{\partial v}{\partial y}\right)$$

where (u, v) are the displacements at the point P during the time interval Δt in the directions of x, y, respectively.

To evaluate the strain tensor components, the strain rates must be known for at least three lines in different directions. As there are random errors in the observations, the least squares adjustment is the optimal solutions, when the number of observations in the different directions from point P is greater than three. In the case of observation:

$$V = Be - \varepsilon$$

In which:

$$\varepsilon^T = (\varepsilon_1\varepsilon_2\varepsilon_3 \ldots \varepsilon_4)$$

$$B = \begin{bmatrix} \cos^2\theta_1 & \sin 2\theta_1 & \sin^2\theta_1 \\ \cos^2\theta_2 & \sin 2\theta_2 & \sin^2\theta_2 \\ \cos^2\theta_3 & \sin 2\theta_3 & \sin^2\theta_3 \\ \cos^2\theta_n & \sin 2\theta_n & \sin^2\theta_n \end{bmatrix} \quad e = \begin{bmatrix} e_{xx} \\ e_{xy} \\ e_{yy} \end{bmatrix}$$

where

V is the residual of the observed values,

B is the coefficient matrix, and

ε is the observed values

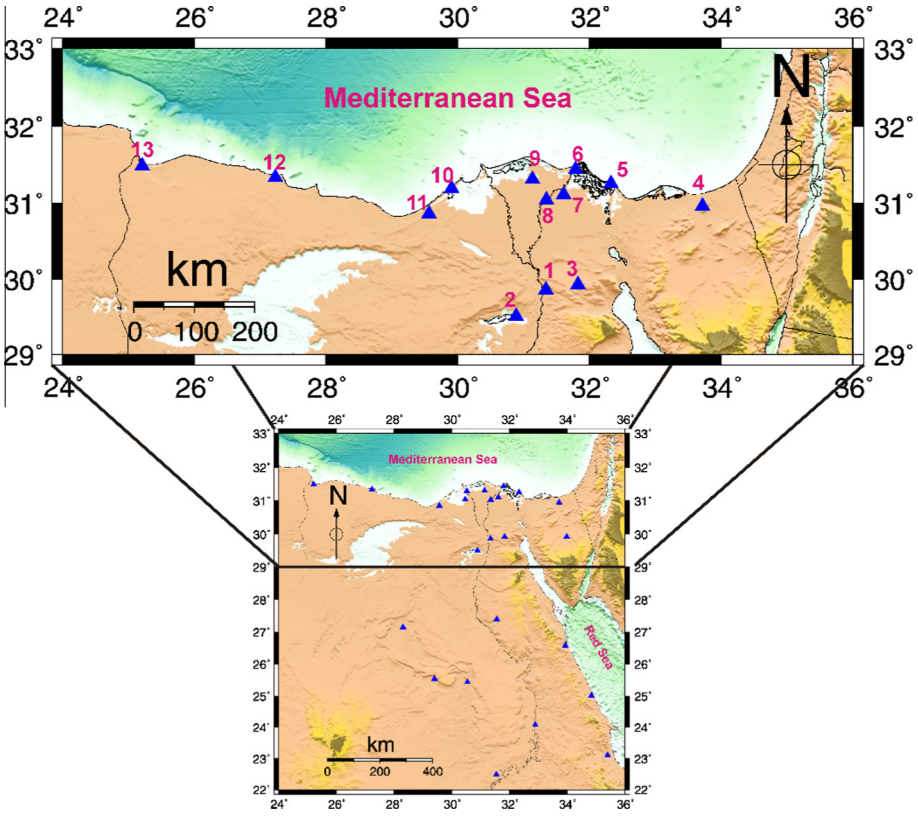

Figure 7 Distribution of the Egyptian Permanent GPS Network (EPGN) with special emphasis on the northern part of Egypt.

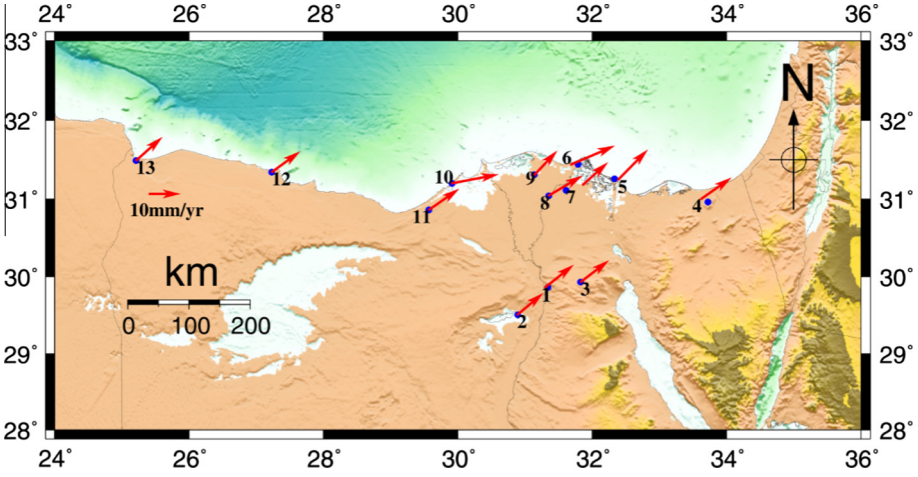

Figure 8 Rate of regional horizontal movements in ITRF 2008 during the period from 2012 to 2014 including the velocity of the African plate.

To make $\varepsilon V^2 = \min$, a least squares method will be applied. The following equation gives the best solution of the system

$$e = (B^T Q_{\varepsilon\varepsilon}^{-1} B)^{-1} \cdot B^T Q_{\varepsilon\varepsilon}^{-1} \varepsilon$$

where Q is the weight matrix obtained from the variance –covariance of coordinates of both observations epochs (Chen, 1991).

Dilatation $\Delta = e_{xx} + e_{yy}$

Pure Shear $\gamma_1 = e_{xx} - e_{yy}$

Engineering Shear $\gamma_2 = 2e_{xy}$

Total shear $\gamma = (\gamma_1^2 + \gamma_2^2)^{1/2}$

Principal strains $\varepsilon_1 = \frac{1}{2}(\Delta + \gamma)$

$$\varepsilon_2 = \frac{1}{2}(\Delta - \gamma)$$

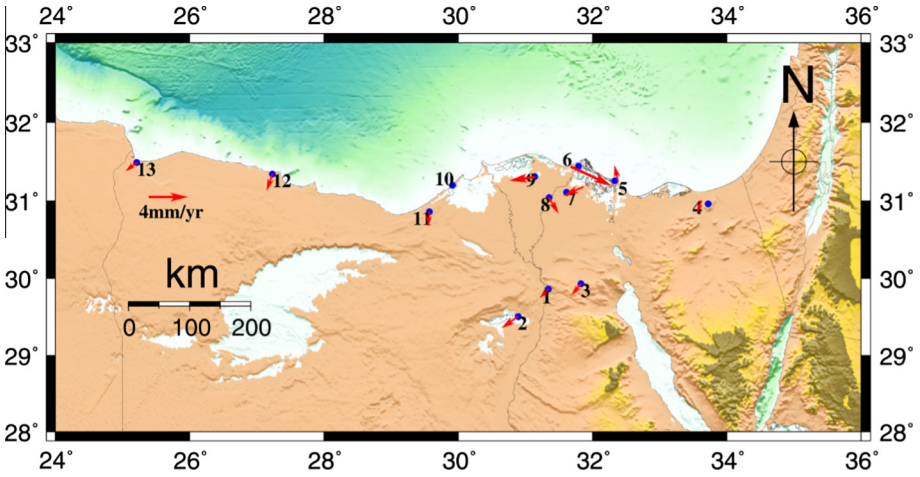

Figure 9 Rate of local horizontal movements in ITRF 2008 during the period from 2012 to 2014.

Table 4 Rate of regional horizontal movements (in m) for northern Egypt during the period from 2012 to 2014.

St.	Longitude	Latitude	VN (m)	VE (m)	δN (m)	δE (m)
1	31.83	29.93	VN (m)	0.0176	0.0001	0.0001
2	30.89	29.51	0.0223	0.0169	0.0001	0.0001
3	31.34	29.86	0.0202	0.0169	0.0001	0.0001
4	33.62	31.11	0.0221	0.0166	0.0001	0.0001
5	32.31	31.25	0.0236	0.0238	0.0001	0.0001
6	31.14	31.31	0.0235	0.0149	0.0002	0.0002
7	31.86	31.18	0.0347	0.0175	0.0002	0.0001
8	31.35	31.04	0.0195	0.0158	0.0001	0.0001
9	31.68	31.44	0.0268	0.0189	0.0002	0.0001
10	29.91	31.20	0.0178	0.007	0.0001	0.0001
11	29.57	30.86	0.0368	0.0164	0.0001	0.0001
12	27.23	31.35	0.0236	0.0161	0.0001	0.0001
13	25.21	31.49	0.0221	0.0182	0.0001	0.0001

Table 5 Rate of local horizontal movements (in m) for the northern Egypt during the period from 2012 to 2014.

St.	Longitude	Latitude	VE (m)	VN (m)	δE (m)	δN (m)
1	31.83	29.93	−0.0022	−0.0021	0.0001	0.0001
2	30.89	29.51	−0.0029	−0.0041	0.0001	0.0001
3	31.34	29.86	−0.0028	−0.0023	0.0001	0.0001
4	33.62	31.11	−0.003	−0.001	0.0001	0.0001
5	32.31	31.25	0.0041	−0.0009	0.0001	0.0001
6	31.14	31.31	−0.0049	0.0105	0.0002	0.0001
7	31.86	31.18	−0.0022	−0.0048	0.0002	0.0001
8	31.35	31.04	−0.004	0.0025	0.0001	0.0001
9	31.68	31.44	−0.0009	−0.0064	0.0002	0.0001
10	29.91	31.20	–	–	–	–
11	29.57	30.86	−0.0036	−0.0003	0.0001	0.0001
12	27.23	31.35	−0.0041	−0.0014	0.0001	0.0001
13	25.21	31.49	−0.0021	−0.0027	0.0001	0.0001

Direction of $\varepsilon_1 \propto = \tan^{-1}\left(\frac{e_{xy}}{\varepsilon_1 - e_{yy}}\right)$

The above mentioned strain parameters are expressed in the deformed body center of gravity. To compute the deformation parameters, the area is divided into several blocks. The parameters of deformation are related to the center of a single block within the network. The horizontal components of the velocity vectors are used to estimate the strain and stress field in the study area. Calculated parameters are the maximum principal strain rate (ε_1), minimum principal strain rate (ε_2), direction of the maximum principal strain rate (α), annual rate of maximum shear strain (γ max) and the dilatation (Δ) (Fuji, 1997). The Fuji software is used for computing the strain in the main block center of gravity and also computing the translation T_x and T_y of these main blocks. This paper used the final analyses from 2012 to 2014.

The estimated total amount of average rate of areal compression strains accumulation is concentrated in the northeastern part of Cairo area during the period from 2012 to 2014 (Fig. 10). Dilatational strains show patches of high and medial values of the compressional strain. Additionally, there are low compressions in the western parts of the area under study. The total amount of maximum shear strain accumulation during the same interval is relatively small and lies in the lowest class (according to Fuji's classifications, 1995) and is prevailed in the area between the Nile valley and the Gulf of Suez (Fig. 11). Medial shear strain part covers some parts in the area while the low shear strain rate covers most parts of the Western Desert. To compare the maximum shear strains with the seismic data, the epicentral distributions are plotted in the same area (Fig. 11). The present period is dominated by compressional strain and shear stress rates and earthquake activities. This indicates that the rocks of those areas could have capability to return back again to its original situation after the occurrence of a remarkable earthquake. This might be due to the restraining and releasing of stresses in those areas. The crustal deformation processes could occur during the

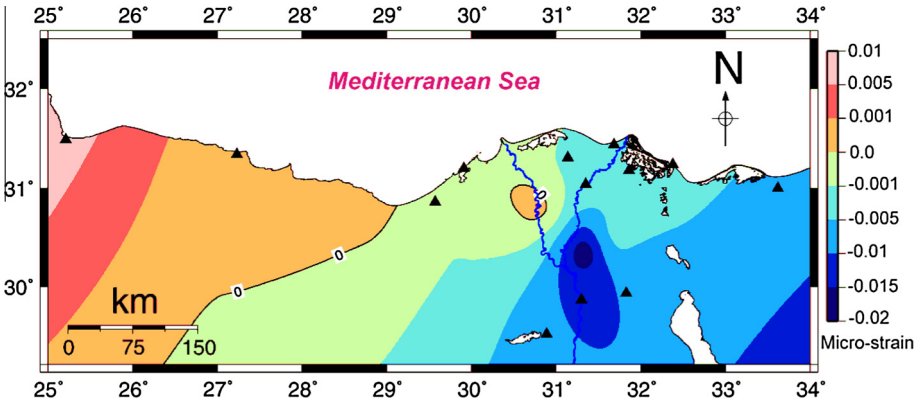

Figure 10 Distribution of the dilatation strain rates in the northern Egypt during the period from 2012 to 2014.

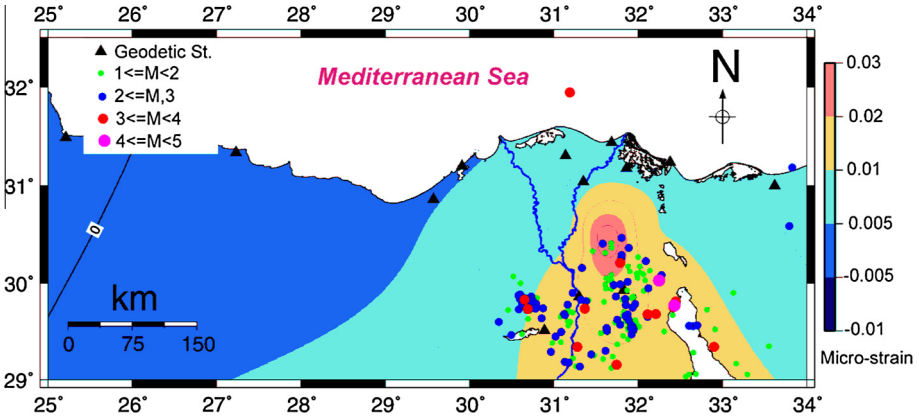

Figure 11 Distribution of the maximum shear strain rates in the northern Egypt during the period from 2012 to 2014.

accumulation and releasing of the energy within the Earth's crust. This means that, those areas have suffered from post-seismic deformation during the present interval. The seismic activity reflects the release of energy accumulated as a result of the pressures accumulated in those areas.

8. Discussion and conclusions

Crustal deformation and seismicity were studied from both seismological and GPS data. The results were compared and combined in order to determine the main characteristics of deformation and hazard estimation for the specified region. By comparing geodetic results with seismic activity in the area, a relation between the accumulated energy releases associated with the earthquake occurrences and the deformation is found. Seismic activity reflects the release of energy accumulated as a result of the pressure accumulated in the area between the Nile valley and Gulf of Suez. The simple blocks model suggests that, northeastern part of Cairo city area is characterized by compressional forces. The results show that the area under study suffers from continuous seismic activity related to the crustal movements taken place along trends of major faults. It must be mentioned that the continuous urban extension and working on large-scale projects may affect the stress regime at the northern part of Egypt and may be a near source for seismic activity. Final compiled output from the seismic and geodetic analysis focuses on the geodynamical regime of the area and it is an attempt to delineate the crustal stress and strain fields.

Obtained results reveal a clear picture about the crustal deformation and their role in the earthquake occurrence. The main points emerging from this study are as follows:

- This study is an attempt to give a clear picture on the crustal deformation and their role in the earthquake occurrence.
- The results are compared and combined in order to determine the main characteristics of deformation and hazard estimation.
- The highest seismicity rates are found at the eastern boundaries of Egypt.
- The seismic activity reflects the release of the energy accumulated as a result of the pressure accumulated in the area between the Nile valley and Gulf of Suez.
- Focal mechanism of some earthquake events recorded during the study period demonstrates mainly normal faulting with strike-slip sense.
- A relation between the accumulated energy releases associated with the earthquake occurrences and the deformation is found.
- Horizontal Velocities in the study area were small.

- Distribution of dilatation in the study area indicates that the eastern part suffered from compression especially in Abu Za'abal area, but the western part suffered from extension.
- Distribution of shear reflects that the most value is found in Suez, Cairo and Ismailia. This triangle is characterized by a high seismicity. The shear value decreases toward the west.

Acknowledgments

The authors would like to thank the staff members of the Crustal Movements Laboratory, Geodynamic Department, NRIAG and the National Seismic Network, NRIAG for helping during data acquisition stage.

References

Abdel-Monem, S.M., Mahmoud, S., Shaker, A., Saad, A., Hamed, M., 2011. Crustal deformation studies in the northern part of Aswan Lake using GPS technique. NRIAG J. Geophys. Spec. Issue, 89–110.

Chen, R., 1991. Horizontal crustal deformations in Finland. Rep. Finish Geodetic Inst. 91, 1.

Dach, R., Hugentobler, U., Fridez, P., Meindl, M. (Eds.), 2007. Bernese GPS Software Version 5.0. Astronomical Institute, University of Bern.

Fuji, Y., 1997. Estimation of continuous distribution of Earth's strain in the Kanto-Tokai district, Central Japan, with the aid of least squares collocation. In: An advanced lectures on geodesy and seismology in Egypt August, 1996-July, 1997. Bulletin of NRIAG, pp. 97–126 (special issue).

Guiraud, R., Bosworth, W., 1997. Senonian basin inversion and rejuvenation of rifting in Africa and Arabia: synthesis and implications to plate-scale tectonics. Tectonophysics 282, 39–82.

Jaeger, J.C., 1964. In: Elasticity Fracture and Flow, with Engineering and Geological Applications. Methuen, London.

Kakkuri, J., Chen, R., 1991. Finnish Geodetic Institute Ilmalankatu IA, SF-00246 Helsinki, Finland.

Moustafa, A., El-Badrawy, R., Gibali, H., 1998. Pervasive E-ENE oriented faults in northern Egypt and their effect on the Development and inversion of prolific sedimentary basis. In: Proceedings of 14th Petroleum Conference, vol 1, Egyptian General Petroleum Corporation, pp 51–67.

Moustafa, A.R., Khalil, M.H., 1990. Structural characteristics and tectonic evolution of north Sinai fold belts. In: Said, R., Balkema, A.A. (Eds.), . In: Geology of Egypt. Rotter Brookfield, pp. 381–389.

McClusky, S., Reilinger, R., Mahmoud, S., Ben Sari, D., Tealeb, A., 2003. GPS constraints on Africa (Nubia) and Arabia plate motions. Geophys. J. Int. 155 (1), 126–138. http://dx.doi.org/10.1046/j. 1365-246X.

Said, R., 1962. The Geology of Egypt. Elsevier Publishing Co., Amsterdam, New York.

Saleh, M., Becker, M., 2013. A new velocity field from the analysis of the Egyptian Permanent GPS Network (EPGN). Arab. J. Geosci. http://dx.doi.org/10.1007/s12517-013-1132-x.

Savostin, L.A., Sibuet, J.-C., Zonenshain, L.P., Le Pichon, X., Roulet, M.J., 1986. Kinematic evolution of the Tethys belt from the Atlantic Ocean to the Pamirs since the Triassic. Tectonophysics 123, 1–35. http://dx.doi.org/10.1016/0040-(86), 90192-7.

Schneider, D., 1982. Complex crustal strain approximation, University of New Brunswick, Fredericton, NB, Institute of Geodesy and Photogrammetry, Swiss Federal, Institute of Technology, Zürich.

Sehim, A., 1993. Cretaceous tectonics in Egypt. Egypt. J. Geol. 37, 335–372.

Suetsugu, D., 1995. Earthquakes Source Mechanism, International Institute of Seismology and Earthquake Engineering (IISEE). Building Research Institute, Japan.

Stern, R.J., Johnson, P., 2010. Continental lithosphere of the Arabian plate: a geologic, petrologic, and geophysical synthesis. Earth-Sci. Rev. 101 (1–2), 29–67. http://dx.doi.org/10.1016/j.earscirev.2010.01.002.